A1117

A novel perspective on accelerated degradation studies of proton exchange membranes

Sven Jovanovic* (1), Robert Rameker (1,2), Jean-Pierre Poc (1,3), Eva Jodat (1), Andre Karl (1), Rüdiger A. Eichel (1,3), Josef Granwehr (1,2)

- (1) IET-1, Forschungszentrum Jülich GmbH, Jülich/Germany;
 - (2) ITMC, RWTH Aachen University, Aachen/Germany;
 - (3) IPC, RWTH Aachen University, Aachen/Germany;
 - *Contact corresponding authors: <u>www.EFCF.com/ContactRequest</u>

Abstract

Accelerated degradation studies are widely applied in research on proton exchange membranes (PEMs) for the investigation of the origins and mechanisms of performance loss for electrolysis or fuel cell applications. In a nutshell, it is reported in literature that degradation in PEMs commonly occurs following Fenton-like reactions, where in situ formed H₂O₂ reacts with transition metal cations to produce radicals. These radicals then alter the ionomer on a chemical level by attacking particularly its polar side chains, causing a loss of functional moieties for proton transport [1]. Fast degradation studies mimic and promote these conditions by subjecting PEMs to high concentrations of H₂O₂ and Fe²⁺ cations at elevated temperatures. However, these studies often exhibit discrepancies when compared to degradation occurring during long-term operation [2].

The presented work attempts to elucidate these discrepancies by i) addressing inconsistencies in accelerated degradation and testing procedures, ii) studying the dependence of degradation on PEM chemistry and structure and iii) utilizing both NMR spectroscopy and SEM microscopy among other techniques for a comprehensive picture. Hereby, solid-state magic angle spinning (MAS) NMR spectroscopy provides information on both chemical and local structural transformations of the PEM, while SEM offers concrete insights into structural changes on a microscopic scale.

The Fenton-like accelerated degradation experiments were optimized for homogeneity and effectiveness by introducing the catalytic iron centers into the PEMs. Additionally, interferences in the analytical techniques were minimized by careful removal of excess reactants after accelerated degradation. The combined analytical techniques reveal that chemical degradation in PEMs is significantly less pronounced than suggested in literature, although differences were observed depending on the type of PEM material. Moreover, organic radicals that form during Fenton-like reactions could not be detected by EPR spectroscopy. However, all samples experienced significant changes in the local structure, as indicated by NMR relaxometry, and microscopic structure, as illustrated by SEM techniques. Thus, instead of chemical degradation, the PEM may be affected on a structural level by mechanical stress due to microscopic gas pockets and macroscopic bubbles forming inside the gas impermeable material.

- [1] L. Ghassemzadeh et al., J. Am. Chem. Soc. 135, 8181–8184 (2013).
- [2] J. Mališ et al., Int. J. Hydrogen Energy 41, 2177–2188 (2016).

Introduction

Green hydrogen is predicted to be a critical resource in a shift towards CO₂-neutral economy, both as an energy carrier and an educt for the chemical and steel industry [1]. Production of green hydrogen needs to be clean, efficient and scalable, thus ion exchange membrane water electrolysis utilizing renewable energy sources are considered a promising technology [2]. While anion exchange membrane water electrolyzers offer an encouraging perspective due to their non-reliance on noble-metal catalysts, their current technology-readiness-level is not sufficient for industrial implementation [3]. Alternatively, proton exchange membrane water electrolyzers (PEMWE) offer the most compelling combination of maturity, performance and efficiency. However, the individual components of PEMWEs, such as bipolar plates, catalysts and proton exchange membranes (PEMs) are associated with a high CAPEX, and therefore, a high durability of these materials is desirable [4]. As a central piece of this technology, a large number of durability studies are focused on PEMs themselves [5]. This study aims to revisit the accelerated degradation experiments on PEM by correlating various analytical techniques, offering both insights on membrane chemistry and structure.

1. Scientific Approach

In literature, degradation of perfluorinated sulfonic acid (PFSA) PEMs is assumed to occur via Fenton or Fenton-like reactions. There, H_2O_2 formed *in situ* at the cathode due to oxygen diffusion reacts with transition metal ions such as Fe^{2+}/Fe^{3+} to form radicals by reductive splitting [6]:

$$Fe^{2+} + H_2O_2 \rightarrow Fe^{3+} + OH^- + OH \bullet$$

HOO• can then form by reaction of the OH• radical with another H_2O_2 , while H• occur due to homolytic splitting of H_2 at the platinum catalyst or by reaction of hydrogen gas with other radicals (fig. 1a). These radicals can then attack the PEM, particularly at side chains, branching points and chain ends, causing a loss of functional moieties that are responsible for proton transport. In accelerated degradation studies these reactions are mimicked by *ex situ* exposure of the PEMs to Fenton's reagents, i.e. an aqueous solution of Fe salts and H_2O_2 at elevated temperatures (fig 1b). Compared to *in situ* conditions, the concentrations of transition metal ions and hydrogen peroxide are significantly higher, and thus, accelerated reaction rates are presumed to occur, degrading the PEM in hours to days as opposed to months and years [7].

An important differentiation of PEM Fenton studies in literature is the method of introducing Fe cations. Fe salts can be solvated in the aqueous solution with H_2O_2 , thus forming the radicals both in the solution itself and in the treated membrane [8]. Alternatively, the sulfonic acid $-SO_3H$ groups of the PEM can be exchanged with iron salt beforehand, thus accumulating all iron centers inside the membrane itself [9]. Subsequent addition of aqueous H_2O_2 solution will only lead to the formation of radicals in the PEM itself. Therefore, this latter method offers a more sophisticated, controlled, and precise Fenton degradation technique. While most accelerated degradation studies are performed on Nafion, a long-side-chain ionomer (fig. 1c), industrial applications favor short-side-chain ionomers such as Aquivion (fig. 1d). Aquivion is considered to be more durable compared to Nafion, as its shorter side chain offers less opportunities for radicals to attack, yet providing lower proton conductivity [10].

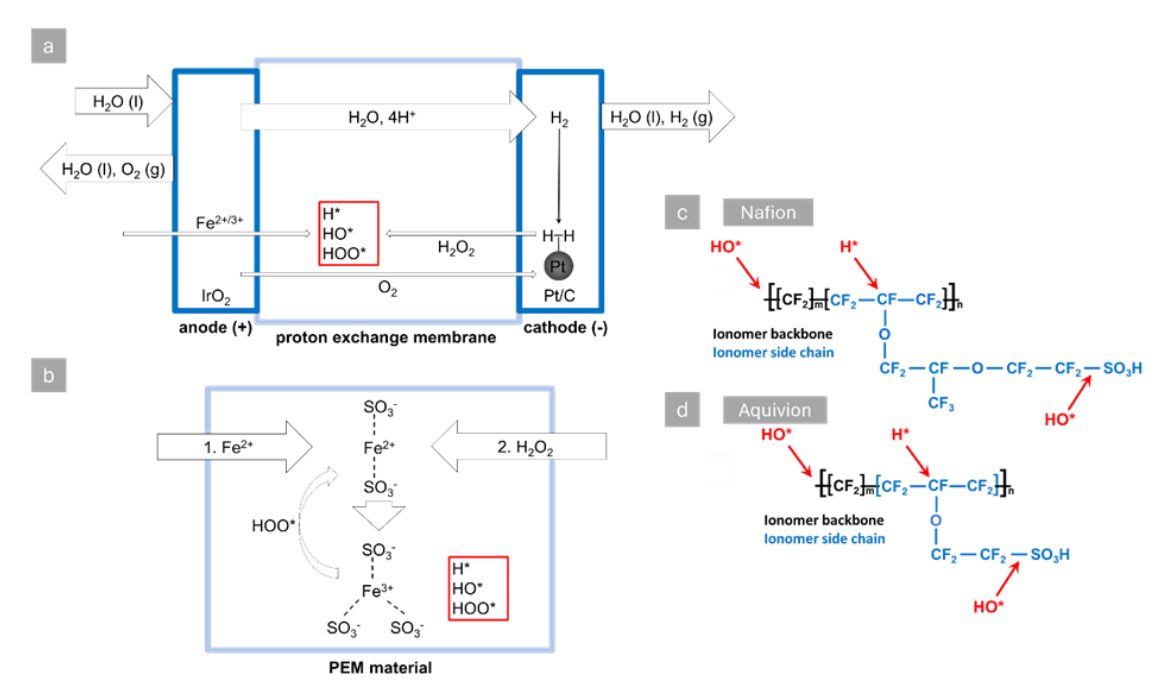


Figure 1: Schematic of the proposed Fenton reaction mechanism in a PEMWE (a) and in an ex_-situ Fenton experiment (b). Arrow widths indicate the relative rates of the associated transport and chemical reactions. Chemical structure of Nafion (c) and Aquivion (d), where proposed radical attack points are highlighted in red.

Published Fenton studies on PEMs utilize a wide variety of analytical tools to investigate degradation occurring in membranes. A common method is the determination of fluorine release rates, often by optical emission spectroscopy, which provides information about fluorine anions in the Fenton solution, as these must originate from the chemical degradation of the PFSA membrane [11]. However, while this technique enables a semi-quantitative evaluation of the degree of degradation, details on its mechanisms and impact are lacking. Therefore, spectroscopic techniques such as solid state NMR, infrared or Raman spectroscopy are exploited in order to provide information on the chemistry of the occurring reactions [12,13]. In particular, all mentioned techniques enable the study of preferential points of radical attacks by determination of relative signal intensities for -OCF₂, -SO₃H or other functional groups. However, reports in literature utilizing these spectroscopic methods exhibit disparities on preferential degradation mechanisms or rates. In case of NMR, the remaining iron cations in the PEM after Fenton treatment in some studies contribute to these uncertainties, as their paramagnetic properties significantly affect the NMR response of the sample [12]. Microscopy, in particular scanning electron microscopy (SEM), are another powerful tool for the examination of PEMs after accelerated degradation tests. [14] Here, all reports agree on the severe morphological changes of membranes after Fenton treatment, with the originally smooth surfaces becoming roughened by the development of tears or pinholes. The extent of these morphological changes strongly depends on the degradation protocol. While these effects are attributed to the described radical attack mechanisms, to our knowledge no correlated study linking these observations to spectroscopic data is published.

This work aims to provide a new perspective on Fenton based accelerated degradation studies of PEMs by establishing a broad and correlated range of analytical results including spectroscopy, microscopy, diffraction and electrochemical methods, and by evaluating the effectiveness of Fenton experiments for the purpose of probing PFSA PEM degradation.

2. Experiments/Calculations/Simulations

Fenton degradation experiments

The pristine Nafion 115 membranes were purchased from Fumatech BWT GmbH (Bietigheim-Bissingen, Germany). The Aquivion E98-15S membranes were purchased from MSE Supplies LLC (Tucson, Arizona, USA). For pretreatment, the samples were exposed to $0.5~M~H_2SO_4$ solution for 5 h at 80 °C. For neutralization, the samples were then treated twice for 1 h in deionized water (DI) water at 80 °C. After each treatment step, the surface of the samples was rinsed with DI water.

For the accelerated stress test, the samples were first mounted in a home-build sample holder and then treated in 1 N H_2SO_4 solution with 1 M $FeSO_4$ for 5 h at 80 °C. The sample holder and the surface of the membrane were then carefully rinsed with DI water and transferred into a 80 °C H_2O_2 solution (30 % v/v in water) for the specified Fenton reaction time. After each 24 h, the H_2O_2 solution was replaced by a fresh H_2O_2 solution.

To remove the catalytic iron after the Fenton reaction, the samples were post-treated twice in $0.5~M~H_2SO_4$ solution for 1 h at 80 °C. For the second repetition, 7 mg Na-EDTA was added per 50 mg membrane material for additional effectiveness of iron removal Afterwards, the samples were washed two times in fresh DI water at 80 °C for 1 h. After each washing step, the samples were rinsed with DI water.

¹⁹F MAS NMR

The ¹⁹F magic angle spinning (MAS) NMR spectra were recorded on a Bruker Avance III HD spectrometer using a Bruker Ascend 400WB (9.6 T, 400 MHz for ¹H) magnet and a dual channel 1.3 mm MAS probe (PH MASDVT 400W1 BL1.3 N-P/H NO-I/E). The experiment temperature was maintained at 25 °C, and the MAS spinning frequency was set to 30 kHz. The ¹⁹F center frequency was adjusted to match the $(CF_2)_n$ signal at -121 ppm, using a spectral width of 199.2 ppm. The recycle delay was set between 1 and 10 s, depending on the T_1 relaxation time of the respective sample. The 90° pulse length was set to 1.1 – 1.2 µs at 45 W radio frequency power.

The raw data were processed using a custom Python script (Python version 3.9). Spectral fitting was performed using Lmfit (version 1.3.3.). Pseudo-Voigt functions were utilized for the fitting of the individual peak components. The deviation of the fit from the data points was kept below 1.5% of the amplitude of the most intense signal.

The relative intensities of the SCF_2/CCF_2 and OCF_2 signal with respect to the $(CF_2)_n$ signal were calculated from the fitted results and normalized to the integral of the $(CF_2)_n$. Errors of the relative signal intensities were calculated via Gaussian error propagation. For this purpose, the root mean square (RMS) of the noise per ppm, $n_{\rm ppm}$, was determined between the range of -100 ppm and -90 ppm. Using

$$n_{\text{signal}} = 4 \sigma n_{\text{ppm}} \tag{6}$$

the error $n_{\rm signal}$ of each signal in the second confidence interval was calculated where σ is its half width at half maximum in units of ppm.

ATR-FTIR spectroscopy

Attenuated total reflection Fourier transform infrared spectroscopy (ATR-FTIR) spectra were collected at ambient temperature on a FT-IR spectrometer (Spectrum 3, FT-IR/FIR Spectrometer, Perkin Elmer, UK) equipped with the proprietary Universal ATR Sampling accessory. Each spectrum was recorded from 650 to 4000 cm⁻¹ at 4 cm⁻¹ resolution and was an average of 32 scans. For each membrane (pristine and Fenton-treated), five different surface locations were measured. The raw data were processed using a custom Python script (v3.11.5).

Raw transmittance (%) data were converted to absorbance via:

Absorbance =
$$-\log_{10}\left(\frac{\text{Transmission}}{100}\right)$$
 (8)

then baseline-corrected using an asymmetric least-squares algorithm. Each baseline-corrected spectrum was normalized to the CF_2 symmetric stretching band, $v_s(CF_2)$, at 1143 cm⁻¹ of the PTFE backbone. The five normalized spectra per sample were averaged to yield a representative spectrum, from which mean normalized peak intensities were extracted and plotted versus Fenton-treatment time to evaluate side-chain alterations.

Scanning Electron Microscopy (SEM) and Cross-Section Preparation

All imaging and cross-sectioning were performed on a Plasma Focused Ion Beam (FIB)-SEM (TESCAN AMBER X, TESCAN). Membranes were mounted on aluminium stubs and dried at ambient conditions for 24 h, then degassed in the microscope chamber for 30 min. Surface micrographs were acquired at 2 kV accelerating voltage and 0.3 nA beam current using an Everhart–Thornley (E-T) secondary-electron detector. Cross-sections were prepared by trench milling with a 30 keV, 25 nA Xe⁺ beam, followed by polishing at 30 kV/5 nA, and imaged under the same 2 kV/0.3 nA conditions.

Quantitative bubble analysis was performed in ImageJ (v1.54p) by counting all visible bubbles within a 3 mm field of view. When densities exceeded ~120 bubbles, counts were limited to a representative subset of 50–120 to maintain accuracy. The resulting radius data were processed in Python and plotted as a filled kernel-density overlay (no extrapolation) using seaborn, with each reaction time rendered in a distinct color.

3. Results

The relative intensities of the individual Nafion and Aquivion groups as a function of Fenton treatment duration can be directly tracked via ¹⁹F MAS NMR (figs. 2a and 2b, respectively). Note that the relative intensities are normalized to the integral of the (CF₂)_n backbone signal and, therefore, only preferential radical attacks can be observed. Based on these results, two conclusions can be drawn. First, Nafion is significantly more prone to preferential radical attacks of the side chain in Fenton degradation compared to Aquivion, which is indicated by the decrease of Nafion SCF₂/CCF₂ signal as a function of Fenton treatment time. For the same experiment duration, only a minor decrease can be observed for Aquivion. Moreover, as the loss of the other side chain and branching point signals is significantly less pronounced or even non-existent, it can be concluded that the decrease of the SCF₂/CCF₂ predominantly stems specifically from the scissoring of the sulfonic acid group. Thus, Fenton radical attacks preferentially occur from the end of the side chain at the functional moiety of the material

For the second conclusion, the relative decrease of functional groups is minor, in particular for Aquivion. This is unexpected as other studies report significant degradation of PEMs even after 24 h due to the elevated radical concentrations during Fenton treatment. We propose that these observations originate from the absent step of iron removal after Fenton treatment, as iron significantly affects line widths and shapes in NMR. The fitting of these altered signals can lead to substantially altered results, as could be confirmed in our own testing. Therefore, to ensure that the fitting results in this study are not affected by residue iron even after washing, the effectiveness of the iron removal with H₂SO₄ and EDTA were confirmed with EPR spectroscopy, where no signature of iron was observed.

The NMR results were confirmed by ATR-IR spectroscopy experiments of Fenton-treated Nafion and Aquivion (figs. 2c and 2d, respectively), where no significant decrease for the polar side chain signals could be observed within margins of errors. At a closer look, however, there were discrepancies for Nafion between the constant ATR-IR -SO₃H band and the slightly diminishing NMR SCF₂/CCF₂ signal. These two observations can be brought

in line by considering ATR-IR as a highly surface sensitive method, while NMR is bulk sensitive. The differences in signal evolution therefore indicate that the exchange Fenton method, where the catalytic iron centers are introduced into the membrane itself, has a significantly higher impact on the inner bulk volume compared to the surface of the PEM.

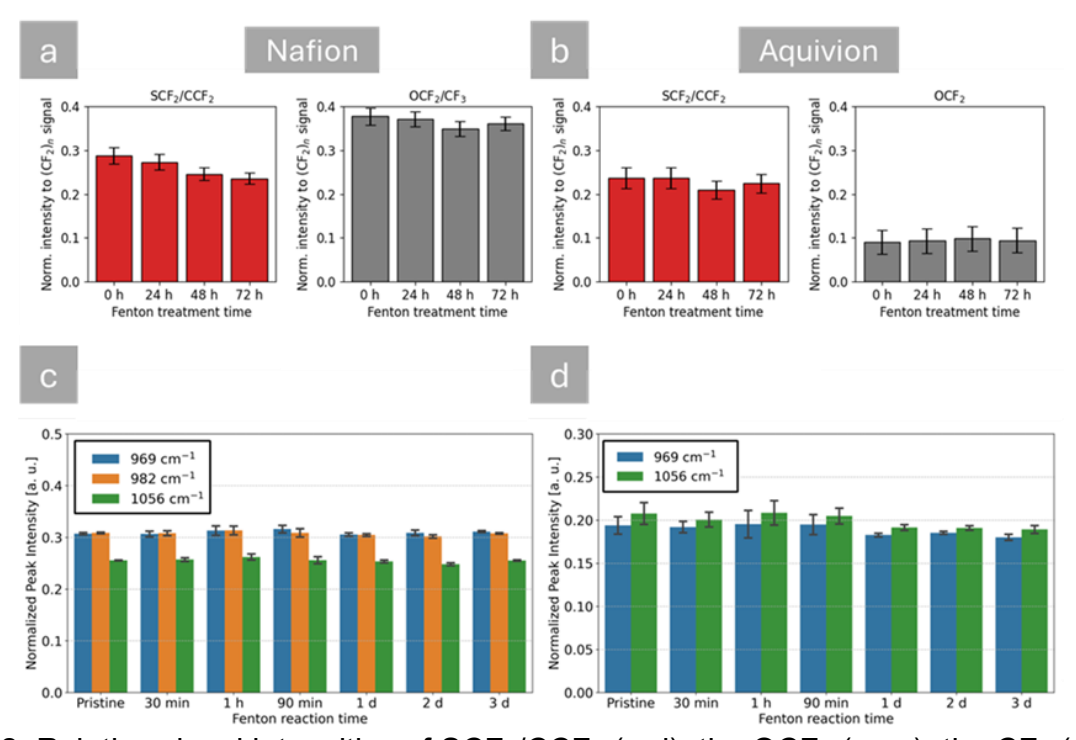


Figure 2: Relative signal intensities of SCF₂/CCF₂ (red), the OCF₂ (grey), the CF_b (orange) and CF_s (teal, Nafion specific) groups obtained from ¹⁹F MAS (30 kHz spinning frequency) measurements of Nafion (a) and Aquivion (b) as a function of Fenton exposure time, normalized to the (CF₂)_n backbone signal. Normalized ATR-IR peak intensities of the 969 cm⁻¹ (C–O–C symmetric stretch mode), 982 cm⁻¹ (additional Nafion-specific C–O–C symmetric stretch mode), and 1056 cm⁻¹ (SO₃⁻ symmetric stretch) bands plotted as a function of Fenton exposure time for Nafion (c) and Aquivion (d).

As treatment of PEMs in Fenton's reagents only produces limited degradation on a chemical scale for this study, SEM was utilized to evaluate the impact on membrane morphology. Here, the changes were significantly more pronounced and could even be observed by eye, as the once transparent membranes turn opaque. Zooming in with SEM, the smooth and featureless surface of pristine Nafion is covered with surface bubbles even after 30 minutes (fig. 3a), which change in radius and density as a function of reaction time (fig. 3c). Specifically, after 30 minutes of Fenton exposure, surface bubbles with radii of ~0.06–0.18 mm emerged. At 90 minutes, bubble density increased clearly while the size distributions narrowed and shifted towards smaller bubbles. Smooth regions persisted between isolated bubbles. After 1 day, smooth areas vanished as bubbles grew and coalesced into irregular, merged features lacking discrete borders. This trend continued for 3 days of reaction time. In both cases, the corresponding histograms in Figure 3c broaden substantially, with measured radii exceeding ~0.20 mm. However, because bubbles coalesced, morphologies lacked well-defined edges, hence true bubble sizes at longer exposures are likely underestimated.

Aquivion showed a similar trend (fig. 3b). However, surface bubbles exhibited smaller radii at significantly narrower size distribution. In addition, the bubbles resisted merging into larger structures, even under prolonged exposure time.

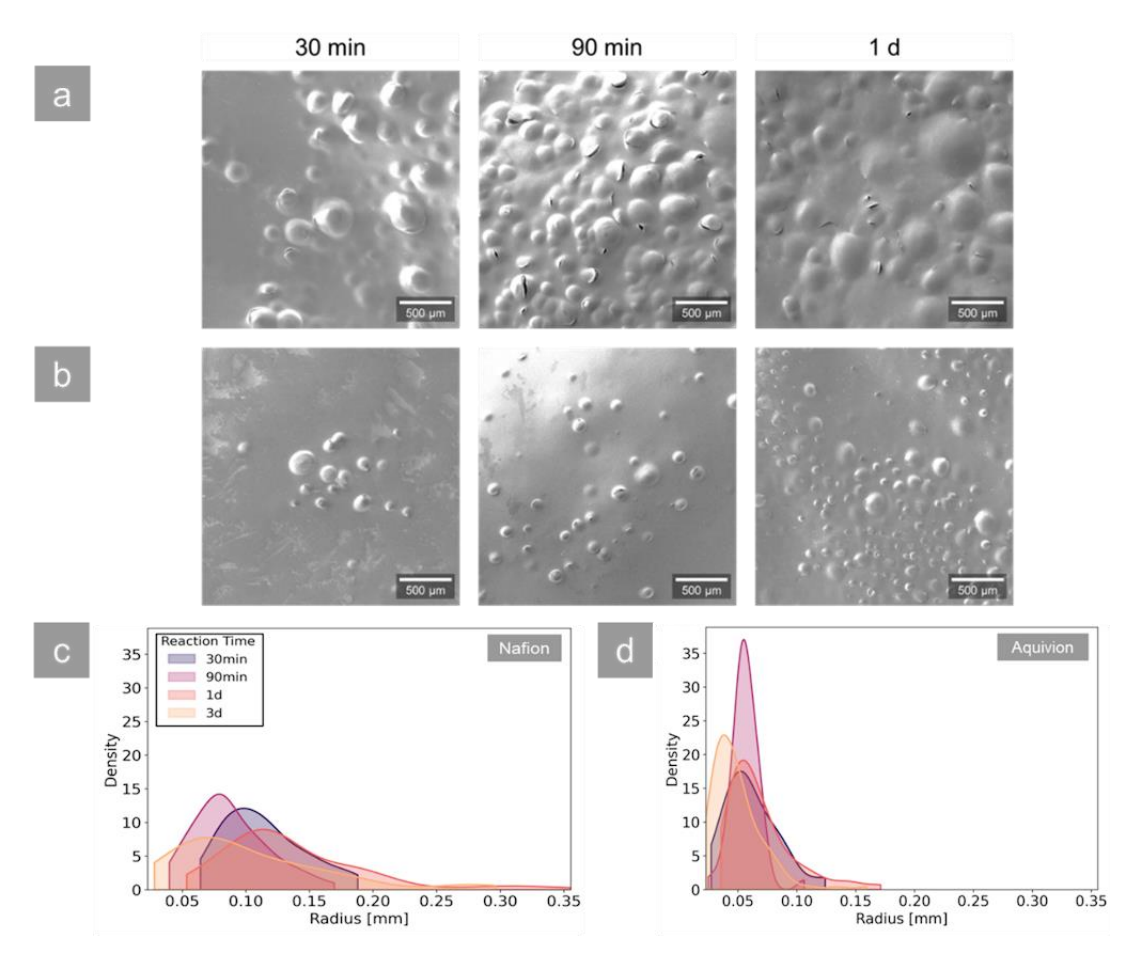


Figure 3: Fenton-induced blistering in PFSA membranes. (a, b) Representative SEM micrographs of (a) Nafion and (b) Aquivion after independent Fenton treatment of 0 min (pristine), 30 min, 90 min, 1 day and 3 days. In both polymers, blister density visibly rises with exposure time. (c, d) Kernel-density estimation of blister radii measured from the corresponding SEM images for (c) Nafion and (d) Aquivion at reaction times of 30 min (purple), 60 min (light purple), 90 min (magenta), 1 day (red) and 3 days (orange).

A closer inspection of the surface protrusions reveals four characteristic morphologies: intact rounded bubbles, burst-cap bubbles, slit-like tears, and collapsed "volcano" structures. Cross-sectional cuts expose underlying voids for these features. Overall, this suggests an inside-out, gas-evolution—driven origin for both Nafion and Aquivion, wherein internal gas generation pushes through the polymer to create these surface protrusions during Fenton_-treatment.

The results are supported by ¹⁹F T_1 relaxation NMR studies, which indicate significant changes in local structure due to a non-trivial evolution of T_1 as a function of reaction time. Here, it can be highlighted that for Nafion, T_1 is affected mainly at prolonged exposure times, while for Aquivion, a strong decrease of T_1 is already observed after 24 hours.

In conclusion, these observations were channeled into a revisited model for ex situ Fenton degradation experiments that is depicted in fig. 4. First, Fe²⁺ is introduced into the membrane, which binds to the SO₃H groups of the PEM (fig. 4a). As H₂O₂ is added to the system, HO* are formed at the Fe²⁺ centers by converting it to Fe³⁺ in a fast reaction (fig. 4b). Previous studies assumed a subsequent attack of the radicals predominantly at the SO₃H side chains, leading to a loss of functionality (fig. 4c). While these reactions occur, the findings in this study indicate that this process is slow. However, long polar side chains such as the ones present in Nafion seem to favor radical attacks compared to short side chain PEMs.

Adversely, a substantially higher impact occurred on the morphology of the membrane. This is correlated to the fast formation of O_2 gas molecules by Fe^{3+} catalyzed reaction of OH^{\bullet} with H_2O_2 (fig. 4d), that, at sufficient production rates, create gas voids in the gas-impermeable PEMs. This causes pressure induced compression inside the membrane, which drives changes in short range order of the membrane, such as crystalline and amorphous regions (fig 4e).

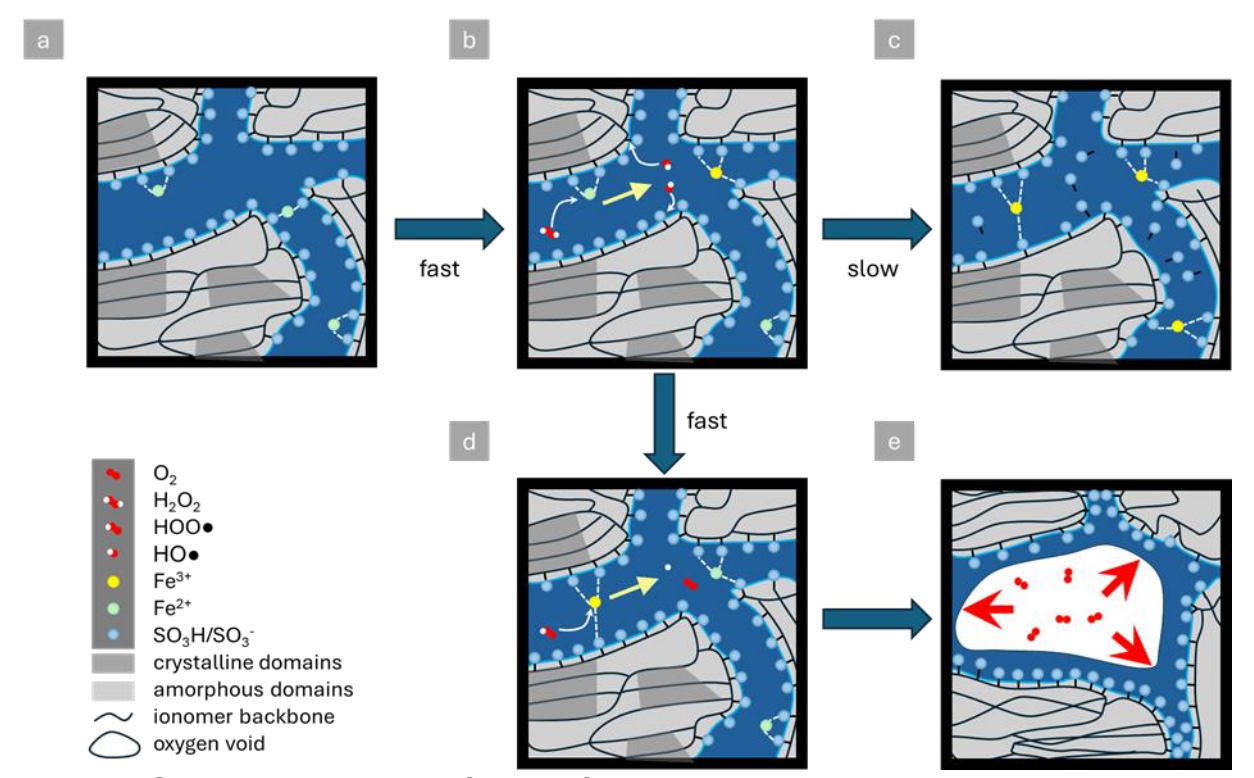


Figure 4: Graphical illustration of the preferred degradation pathway during the Fenton-treatment. (a) During pre-treatment with an acidic FeSO₄ solution, Fe²⁺ ions are coordinated by SO₃-groups, increasing charge transfer conductivity. (b) The addition of a 30% H₂O₂ solution forms hydroxyl (HO*) radicals while Fe²⁺ is oxidized to Fe³⁺. (c) These highly reactive radicals attack the ionomer, degrading sulfonic acid groups, as suggested by ¹⁹F MAS-NMR and ATR-IR data. (d) However, the Fenton-treatment appears to impact the morphology of the ionomer more than its chemical structure. Oxygen molecules are formed in several side reactions of the Fenton mechanism, for example through the splitting of hydroperoxyl (HOO*) radicals with Fe³⁺. (e) If oxygen is formed at high reaction rates, it cannot escape the ionomer's hydrophilic pore structure immediately. Consequently, gas voids form in the pores, increasing their size as more oxygen is

References

produced. The solid phase of the membrane is compressed by the pressure originating from the gas voids, affecting the disorder and crystallinity within the ionomer.

- [1] A. Bhaskar et al., Decarbonizing primary steel production: Techno-economic assessment of a hydrogen based green steel production plant in Norway. Journal of Cleaner Production (350), 2022.,
- [2] P.-A. Le et al., The current status of hydrogen energy: an overview. RSC Advances (13), 2023.
- [3] N. Du et al., Anion-Exchange Membrane Water Electrolyzers. Chemical Reviews (122), 2022.



- [4] J. Proost, State-of-the art CAPEX data for water electrolysers, and their impact on renewable hydrogen price settings. International Journal of Hydrogen Energy (44), 2019.
- [5] F. N. Khatib et al., Material degradation of components in polymer electrolyte membranes (PEM) electrolytic cell and mitigation mechanisms: a review. Renewable and Sustainable Energy Reviews (111), 2019.
- [6] E. Wallnöfer-Ogris et al., A review on understanding and identifying degradation mechanisms in PEM water electrolysis cells: Insights for stack application, development, and research. International Journal of Hydrogen Energy (65), 2024.
- [7] S. H. Frensch et al., Impact of iron and hydrogen peroxide on membrane degradation for polymer electrolyte membrane water electrolysis: Computational and experimental investigation on fluoride emission. Journal of Power Sources (420), 2019.
- [8] T. Kinumoto et al., Durability of perfluorinated ionomer membrane against hydrogen peroxide. Journal of Power Sources (158), 2006.
- [9] A. Bosnjakovic et al., Nafion Perfluorinated Membranes Treated in Fenton Media: Radical Species Detected by ESR Spectroscopy. Journal of Physical Chemistry B (108), 2004.
- [10] S- Shahgaldi et al., The impact of short side chain ionomer on polymer electrolyte membrane fuel cell performance and durability. Applied Energy (217), 2018.
- [11] V. Prabhakaran et al., Investigation of PEM Degradation Kinetics and Degradation Mitigation Using In Situ Fluorescence Spectroscopy and Real-Time Monitoring of Fluoride-Ion Release. ECS Transactions (50), 2013.
- [12] L. Ghassemzadeh et al., Evaluating chemical degradation of proton conducting perfluorosulfonic acid ionomers in a Fenton test by solid-state ¹⁹F NMR spectroscopy. *Journal of Power Sources* (196), 2011.
- [13] F.C. Teixeira et al., Chemical stability of new nafion membranes doped with bisphosphonic acids under Fenton oxidative conditions. International Journal of Hydrogen Energy (48), 2023.
- [14] S. Kundu et al., Comparison of two accelerated Nafion[™] degradation experiments. Polymer Degradation and Stability (93), 2008.

Keywords: EFCF2025, H₂, LowTemp. Fuel Cells & Electrolysers, PEMs, degradation, Fenton, analytics

Remark: This work is licensed under Creative Commons Attribution 4.0 International